Defect–Defect Correlation Functions, Generic Scale Invariance, and the Complex Ginzburg–Landau Equation

Bruce W. Roberts, Eberhard Bodenschatz, and James P. Sethna

Laboratory of Atomic and Solid–State Physics,

Cornell University,

Ithaca, NY 14853–2501.

Abstract

We present a calculation of defect–defect correlation functions in the defect turbulence regime of the complex Ginzburg–Landau equation. Our results do not agree with the predictions of generic scale invariance. Using the topological nature of the defects, we prove that defect–defect correlations cannot decay as slowly as predicted by generic scale invariance

Spatiotemporal chaos occurs in extended systems with many interacting degrees of freedom [1]. Typically, it appears in nonequilibrium pattern–forming systems slightly above their threshold of instability [2]. The study of spatiotemporal chaos has been advanced by the development of experimental systems which are precisely controlled and have a large aspect ratio [3–5]. Such systems have large statistically homogeneous regions relatively free from boundary effects. A key question to address is whether such regions can be described in terms of hydrodynamic–like theories, focusing on collective behaviors and long–wavelength descriptions. We wish to address an aspect of this question by considering the coherent structures known as topological defects (or spirals or vortices) in a system that exhibits spatiotemporal chaos: the complex Ginzburg–Landau equation [6]. This equation describes the slowly varying amplitude and phase in an extended system which undergoes a Hopf bifurcation to an oscillating and spatially uniform or oscillatory and spatially periodic state. The equation exhibits many interesting patterns, but we will restrict our investigation to the Benjamin–Feir unstable (or defect turbulent) regime [7], in which topological defects occur in the context of spatiotemporal chaos. Other systems, such as Rayleigh–Bénard convection [3], electrohydrodynamic convection in liquid crystals [4], capillary ripples [5], cardiac tissue [8], and chemical reactions [9], can exhibit similar defect–turbulent behavior. In this letter, we will examine the defect–defect correlation functions and relate them to the ideas of generic scale invariance, which is a theory for describing nonequilibrium systems with conservation laws. We will see that our results do not match the predictions of generic scale invariance [10]. Finally, we will prove that the generic predictions cannot be correct for topological defect correlations.

The complex Ginzburg–Landau equation is given by

$$\partial_t A = A - (1+ic)|A|^2 A + (1+ib_x)\frac{\partial^2 A}{\partial x^2} + (1+ib_y)\frac{\partial^2 A}{\partial y^2} \tag{1}$$

where A is a complex field in two dimensions. This equation can have topological defect solutions where $A = 0$ (both ReA and ImA are zero) [6,11]. These defects can occur in either static arrangements or in dynamic ones called defect turbulence, where defects are

continuously nucleated and annihilated in pairs and are moving about. We wish to focus on the latter case, the Benjamin–Feir turbulent instability regime [7], which occurs when $1+b_\alpha c < 0$. In this region of parameter space, all periodic solutions of the complex Ginzburg–Landau equation are unstable. For comparison with the ideas of generic scale invariance [10], we will focus on the anisotropic case $b_x \neq b_y$.

We note that the topological defects come in two varieties. The type of defect depends on how the phase of A changes as we go counterclockwise once around the defect. A defect with a phase jump of 2π has a topological charge of $+1$, while one with a jump of -2π has a topological charge of -1. This is analogous to the right–handed and left–handed single–armed spirals in Rayleigh–Bénard convection. We let $\rho_+(\mathbf{r})$ equal the density of $+1$ defects and $\rho_-(\mathbf{r})$ equal the density of -1 defects. We can then define a "topological" order parameter, $\rho(\mathbf{r}) \equiv \rho_+(\mathbf{r}) - \rho_-(\mathbf{r})$, which is just the density of the defects weighted by their topological charge. This order parameter is conserved in a system with periodic boundary conditions: $\int_V \rho(\mathbf{r}) d\mathbf{r} = 0$, as defects can only be created or destroyed in $\pm$ pairs. We focus on the order parameter $\rho(\mathbf{r})$ as an effective coarse–grained field, which we conjecture can be described by some hydrodynamic equation of motion.

In equilibrium systems, spatial correlations typically decay exponentially. For nonequilibrium systems (such as those with an external driving force) the situation can be quite different. For nonequilibrium systems with a conservation law and external noise, spatial correlation functions can decay algebraically. It has been suggested that this algebraic decay is expected to occur for a broad range of conditions, and it has been called "generic scale invariance" [10]. Some extended deterministic chaotic systems also exhibit algebraic decay [12–14]. In at least one of these examples the chaotic fluctuations appear to play the same role as stochastic noise [12]. The complex Ginzburg–Landau equation would seem to satisfy the criterion for generic scale invariance. It shows nonequilibrium behavior since it cannot be derived from an underlying potential (*i. e.* it is non–relaxational). In a system with periodic boundary conditions, the topological order parameter $\rho(\mathbf{r})$ is conserved. Finally, we conjecture that the chaotic noise in our system plays the role of stochastic noise.

With this set of conditions, we could have a hydrodynamic equation for the conserved order parameter of the form

$$\partial_t \rho(\mathbf{r},t) = \Gamma\{\rho(\mathbf{r},t)\} + \eta(\mathbf{r},t) \tag{2}$$

where Γ is a general conserving operator on ρ, such as $\Gamma_0\nabla^2 + \Gamma_1(\nabla^2)^2 + \Gamma_{2x}\partial_x^4 + \Gamma_{2y}\partial_y^4$. It can also contain nonlinear terms (*e. g.* $\nabla \cdot [(\nabla^2\rho)(\nabla\rho)]$) . The stochastic noise term η is determined by:

$$\langle \eta(\mathbf{r},t) \rangle = 0 \tag{3a}$$

$$\langle \eta(\mathbf{r},t)\ \eta(\mathbf{r}\,',t') \rangle = D\delta(\mathbf{r}-\mathbf{r}\,')\delta(t-t'), \tag{3b}$$

where D must be composed of differential operators for our strictly conserved order parameter. This conserving noise term represents the effect of the chaotic fluctuations in the complex Ginzburg–Landau equation. There is evidence from the mapping of the Kuramoto–Shivashinskii equation to the Kardar–Parisi–Zhang equation [15] and from coupled map lattices [12] that this identification of spatiotemporal chaotic fluctuations with stochastic noise is not unreasonable.

For systems with nonconserving noise (*i.e.* D is a constant), equation (2) is expected to always give rise to power law decays in the two point correlation function $G_\rho(\mathbf{r}) \equiv \langle \rho(\mathbf{r})\rho(\mathbf{0})\rangle$, as well as in higher order correlation functions. For systems with conserving noise (*e. g.* $D = D_1\nabla^2$) the situation is somewhat more complicated [10]. If the system is isotropic, then one obtains exponential decays in $G_\rho(\mathbf{r})$, but power law decays occur in higher order correlation functions. Systems which break the isotropy give rise to algebraic decay in $G_\rho(\mathbf{r})$. For systems with cubic symmetry, one expects $G_\rho(\mathbf{r}) \sim 1/r^{d+2}$ for large r. For systems which break the cubic symmetry one expects $G_\rho(\mathbf{r}) \sim 1/r^d$. We will be working in the last regime, where in a two–dimensional system with broken square symmetry, generic scale invariance predicts that

$$G_\rho^{generic}(\mathbf{r}) = \langle \rho(\mathbf{r})\rho(\mathbf{0})\rangle \sim 1/r^2 \tag{4}$$

for large r [10]. We shall compare this prediction to the results from our numerics.

Before we consider the numerics, we should provide some caveats. The ideas behind generic scale invariance depend upon showing that the nonlinearities are irrelevant in a renormalization group sense. It has proven notoriously difficult to treat topological defects in a perturbative manner. An example of this is the Kosterlitz–Thouless transition [16]. We also note that generic scale invariance requires short–ranged interactions. There is some evidence that this is true for the defects in the complex Ginzburg–Landau equation [17], but collective effects might be important. Finally, the mapping of chaotic fluctuations to stochastic noise could break down.

We have numerically solved equation (1) with periodic boundary conditions in the turbulent regime using a pseudo–spectral code. The system is 240×240 in real space, with 360 Fourier harmonics in both directions. We use the parameter values $c = 1.5$, $b_x = -0.75$, and $b_y = -3.0$. The time step used was $\Delta t = 0.02$. We initially "equilibrate" from a state with two oppositely charged defects to a state with fluctuations about some average number of defects. This takes typically 5000 time steps. We note that the defects do not form bound pairs. When a pair is created, the defects tend to move apart, and when they eventually annihilate, they usually do so with a defect other than their initial partner. This illustrates that we aren't in a Kosterlitz–Thouless bound pair phase [16]. In figure 1 we show a snapshot of part of our system. To find the defects in our system, we examine the change in the phase of A as we go counterclockwise around each plaquette on our lattice in real space. A change of 0 signifies that the plaquette does not contain a defect, while changes of $\pm 2\pi$ reveal that a defect exists in the plaquette. Once we have found the defects, we can then proceed to calculate $n(t)$, the total number of defects in the system, and $G_\rho(\mathbf{r})$. To do the averaging, we have run for $750,000$ time steps (one month of CPU time on an IBM RS/6000 model 550: locating the defects is the time consuming part). We only sample $G_\rho(\mathbf{r})$ and $n(t)$ every 10 time steps, because adjacent time steps are not statistically independent. We have calculated that $\langle n(t)n(0)\rangle - \langle n\rangle^2 \sim e^{-t/\tau}$, with $\tau \sim 115$ time steps. It has been predicted [18] that the probability of finding a particular value of n in the system is given by

$P(n) \sim e^{-(n-\langle n\rangle)^2/2\langle n\rangle}$. We have calculated the various moments of our distribution $P(n)$, and we find $\langle n\rangle = 422.8\pm0.3$, $\sigma^2 = 397\pm30$, and a skewness of 0.014 and kurtosis of -0.026, which is in good agreement with the predictions. In figure 2 we present the results for $G_\rho(\mathbf{r})$ with $\mathbf{r}$ in both the $\hat{x}$ and $\hat{y}$ directions. For both directions the typical nearest neighbor is of the opposite sign: the charges are thus screened. Similar behavior for vortices in random wave fields has been observed [19]. In figure 3 we show log–log plots of $|G_\rho(r)|$. We also show lines that represent the slope $|G_\rho(r)|$ should have if it decayed like $1/r^2$. We note that at the right edge of the figure, we have reached the point where our data is dominated by statistical noise. It is clear that neither direction shows the expected $1/r^2$ decay. Our results are at variance with the predictions of generic scale invariance. We expect that the theory is not applicable to these sorts of systems with strong constraints placed on them due to the topological nature of the order parameter. We can't explicitly determine an equation like equation 2 for the defects, but we can discuss the results for $|G_\rho(r)|$ from the viewpoint of topological constraints. We will show how these constraints place bounds upon the decay rate of the correlation function.

We define the excess order parameter in a region to be

$$\delta\rho_L \equiv \left| \int_{\mathbf{r}\in B(L)} \left(\rho(\mathbf{r}+\mathbf{r}_0) - \rho_0\right) d\mathbf{r} \right| . \tag{5}$$

where $B(L)$ represents a circle of radius L about a point $\mathbf{r}_0$, which we take as $\mathbf{r}_0 = \mathbf{0}$ due to translational invariance. For nontopological objects, the constraint is given by $\delta\rho_L \leq a_1 L^2$, where a_1 is some numerical constant. The excess of a nontopological object in a particular region must scale as the volume of that region, since each individual object occupies a fixed volume. For topological objects, this constraint is different, *i. e.* $\delta\rho_L \leq a_2 L$, where a_2 is again some numerical constant. The constraint arises from the fact that any excess of topological defects in a region must be detectable simply by traversing the perimeter of that region. Each topological defect has an "arm" with characteristic width that must pass through the perimeter of the region. Examples of this are the spiral arms of the defects in Rayleigh–Bénard convection, extra rows of atoms for dislocations in crystals, and in our

case lines of $ReA = 0$ and $ImA = 0$. When a region contains the maximum excess number of defects allowed, each of these lines takes up a fixed amount of the perimeter of the region. Since the maximum excess number of topological objects scales linearly with the number of lines, and the number of lines scales as the perimeter of the region, we must have that the maximum excess number of topological objects scales as the linear size L of the region.

If we assume that the correlation function $G_\rho(\mathbf{r})$ decays at the same asymptotic rate independent of the direction of $\mathbf{r}$, *i.e.* $G_\rho(\mathbf{r}) \sim f(\theta)g(r)$, where $g(r) \sim 1/r^\alpha$ for large r, then with this constraint we can show for two dimensions that α must be greater than 2. This result also requires that $\int_0^{2\pi} f(\theta)d\theta \neq 0$, which we expect to be true except for special cases. An example of such a correlation function satisfying both assumptions is given in reference [20]. To show that $\alpha > 2$, we begin by squaring equation (5) and averaging the result (over the noise or over time and space). This gives us the constraint equation

$$\langle \delta\rho_L^2 \rangle = \int_{\mathbf{r}\in B(L)} \int_{\mathbf{r}\,'\in B(L)} d\mathbf{r}d\mathbf{r}\,' G_\rho(\mathbf{r}-\mathbf{r}\,') \leq a^2 L^2. \tag{6}$$

Separating $G_\rho(\mathbf{r}-\mathbf{r}\,')$ into radial and angular components yields

$$\langle \delta\rho_L^2 \rangle = \frac{1}{2\pi} \int_0^{2\pi} f(\theta)d\theta \int_0^{2L} g(R)w(R)dR \tag{7}$$

where we can derive that

$$w(R) = 4\pi R L^2 \left[\cos^{-1}\left(\frac{R}{2L}\right) - \frac{R}{2L}\sqrt{1-\left(\frac{R}{2L}\right)^2} \right]. \tag{8}$$

This result is obtained by considering how often $|\mathbf{r}-\mathbf{r}\,'| = R$ when $\mathbf{r} \in B(L)$ and $\mathbf{r}\,' \in B(L)$, *i. e.*

$$w(R) = \int_{\mathbf{r}\in B(L)} \int_{\mathbf{r}\,'\in B(L)} d\mathbf{r}d\mathbf{r}\,' S(R)\delta(\mathbf{r}-\mathbf{r}\,'-\mathbf{R}), \tag{9}$$

where $S(R) = 2\pi R$ (the circumference of the circle of radius R). From this definition $w(R)$ can be calculated by writing the δ–function in integral form, and then performing the resulting integrals. By assuming that $G_\rho(\mathbf{R})$ exhibits its asymptotic behavior outside of some $R > r_{min}$, we can split the radial integral in equation (7) into two parts:

$$\int_0^{2L} g(R)w(R)dR = \int_{r_{min}}^{2L} + \int_0^{r_{min}} g(R)w(R)dR. \tag{10}$$

We can then examine the large L limit of $\langle \delta\rho_L^2 \rangle$ for various values of the power law exponent α. By rescaling all lengths by $2L$ and then expanding $w(R)$ about small R, we can show that the leading order behaviour of $\langle \delta\rho_L^2 \rangle$ is

$$\begin{aligned}
&\alpha < 2 : \langle \delta\rho_L^2 \rangle \sim L^2 L^{2-\alpha} \\
&\alpha = 2 : \langle \delta\rho_L^2 \rangle \sim L^2 \log(L) \\
&\alpha > 2 : \langle \delta\rho_L^2 \rangle \sim L^2.
\end{aligned} \tag{11}$$

Within our assumptions, this result means that for topological objects the results of generic scale invariance cannot hold, since the constraint given by equation (6) would be violated. In fact, what we have provided is a bound on α. For topological objects α must be strictly greater than 2. Generic scale invariance predicts $\alpha = 2$. The simple geometric nature of topological objects prevents them from having correlation functions that decay as certain power laws. An added conclusion is that if the topological objects form ordered states, they must be of the antiferromagentic variety (*e.g.* alternating $+$ and $-$ vortices) in at least one direction, in order to satisfy the topological constraint. An example of such a state is given in [21].

In our analysis we have only considered the largest possible fluctuations. We expect these fluctuations to be rare, and hence expect a faster decay than the bound we provide. As an analogy, for nontopological objects the analysis presented here would predict that the correlation function can be at most a constant for large r; in practice systems like spins or atoms have connected correlation functions that decay to zero, either as power laws or as exponentials. We expect similarly for real topological objects the decay of the correlation functions will be faster than the bound given here. Numerically, we have found that we are indeed far from saturating this bound.

We would like to thank P. C. Hohenberg, J. F. Marko, and M. E. J. Newman for helpful conversations. This work was partly funded by the Hertz Foundation (BWR), the NSF

under grant DMR–91–18065 (BWR, JPS), and the Alfred P. Sloan Foundation (EB). We also thank the Cornell Materials Science Center for the use of its computational resources.

REFERENCES

[1] M. C. Cross and P. C. Hohenberg, Science **263**, 1569 (1994).

[2] M. C. Cross and P. C. Hohenberg, Reviews of Modern Physics **65**, 851 (1993).

[3] E. Bodenschatz, J. DeBruyn, G. Ahlers, and D. Cannell, Phys. Rev. Lett. **67**, 3078 (1991); Stephen W. Morris, Eberhard Bodenschatz, David S. Cannell, and Guenter Ahlers, Phys. Rev. Lett. **71**, 2026 (1993).

[4] S. Kai and K. Hirakawa, Prog. Theor. Phys. Suppl., **64**, 212 (1978); E. Braun, S. Rasenat, and V. Steinberg, Europhys. Lett. **15**, 597 (1991).

[5] N. B. Tufillaro, R. Ramashankar, and J. P. Gollub, Phys. Rev. Lett. **62**, 422 (1989).

[6] P. Coullet, L. Gil, and J. Lega, Phys. Rev. Lett. **62**, 1619 (1989); Physica D **37**, 91 (1989); Igor Aranson, Lorenz Kramer, and Andreas Weber, Phys. Rev. Lett. **72**, 2316 (1994).

[7] A. C. Newell, in *Nonlinear Wave Motion*, edited by A. C. Newell (American Mathematical Society, Providence, R. I., 1974).

[8] J. M. Davidenko *et al.*, Nature **355**, 349 (1993).

[9] Q. Ouyang and H. L. Swinney, Chaos **1**, 411 (1991).

[10] G. Grinstein, D.–H. Lee, and Subdir Sachdev, Phys. Rev. Lett. **64**, 1927 (1990); G. Grinstein, J. Appl. Phys. **69**, 5441 (1991); G. Grinstein, C. Jayaprakash, and J. E. S. Socolar, Phys. Rev. E **48**, R643 (1993).

[11] P. S. Hagan, SIAM J. Appl. Math. **42**, 762 (1982); E. Bodenschatz, A. Weber, and L. Kramer, in *Nonlinear Wave Processes in Excitable Media*, A. Holden, M Markus, and H. Othmer, eds. (Plenum Press, New York, 1991).

[12] Ravi Bhagavatula, G. Grinstein, Yu He, and C. Jayaprakash, Phys. Rev. Lett. **69**, 3483 (1992).

[13] D. Hansel and H. Sompolinsky, Phys. Rev. Lett. **71**, 2710 (1993).

[14] M. Eisele, Physica D **48**, 295 (1991).

[15] C. Jayaprakash, F. Hayot, and Rahul Pandit, Phys. Rev. Lett. **71**, 12 (1993).

[16] P. Minnhagen, Rev. Mod. Phys. **59**, 1001 (1987).

[17] Igor S. Aranson, Lorenz Kramer, and Andreas Weber, Phys. Rev. E **47**, 3231 (1993).

[18] L. Gil, J. Lega, J. L. Meunier, Phys. Rev. A **41**, 1138 (1990).

[19] N. Shvartsman and I. Freund, Phys. Rev. Lett. **72**, 1008 (1994).

[20] Z. Cheng, P. L. Garrido, J. L. Lebowitz, and J. L. Vallés, Europhys. Lett. **14**, 507 (1991).

[21] A. Weber, E. Bodenschatz, and L. Kramer, Adv. Mater. **3**, 191 (1991).

FIGURES

FIG. 1. Snapshot of a 70×70 region. The solid lines are where $ReA = 0$, and the dashed lines are where $ImA = 0$. Filled circles ($\bullet$) are vortices with topological charge $+1$, and the open circles ($\circ$) have charge -1.

FIG. 2. $G_\rho(\mathbf{r})$ versus r. The solid line is for the $\hat{x}$ direction, while the dashed line is for the $\hat{y}$ direction. Also shown is a line for $G = 0$. Note that G attains its asymptotic limit of 0 from different sides of this line.

FIG. 3. Log–log plot of $|G_\rho(\mathbf{r})|$ versus r. The solid line corresponds to the $\hat{x}$ direction and the dashed line to the $\hat{y}$ direction. Also shown is a line with slope that would correspond to $|G_\rho(r)| \sim 1/r^2$. Note also the break in the line for the $\hat{y}$ direction which corresponds to the zero crossing of G.

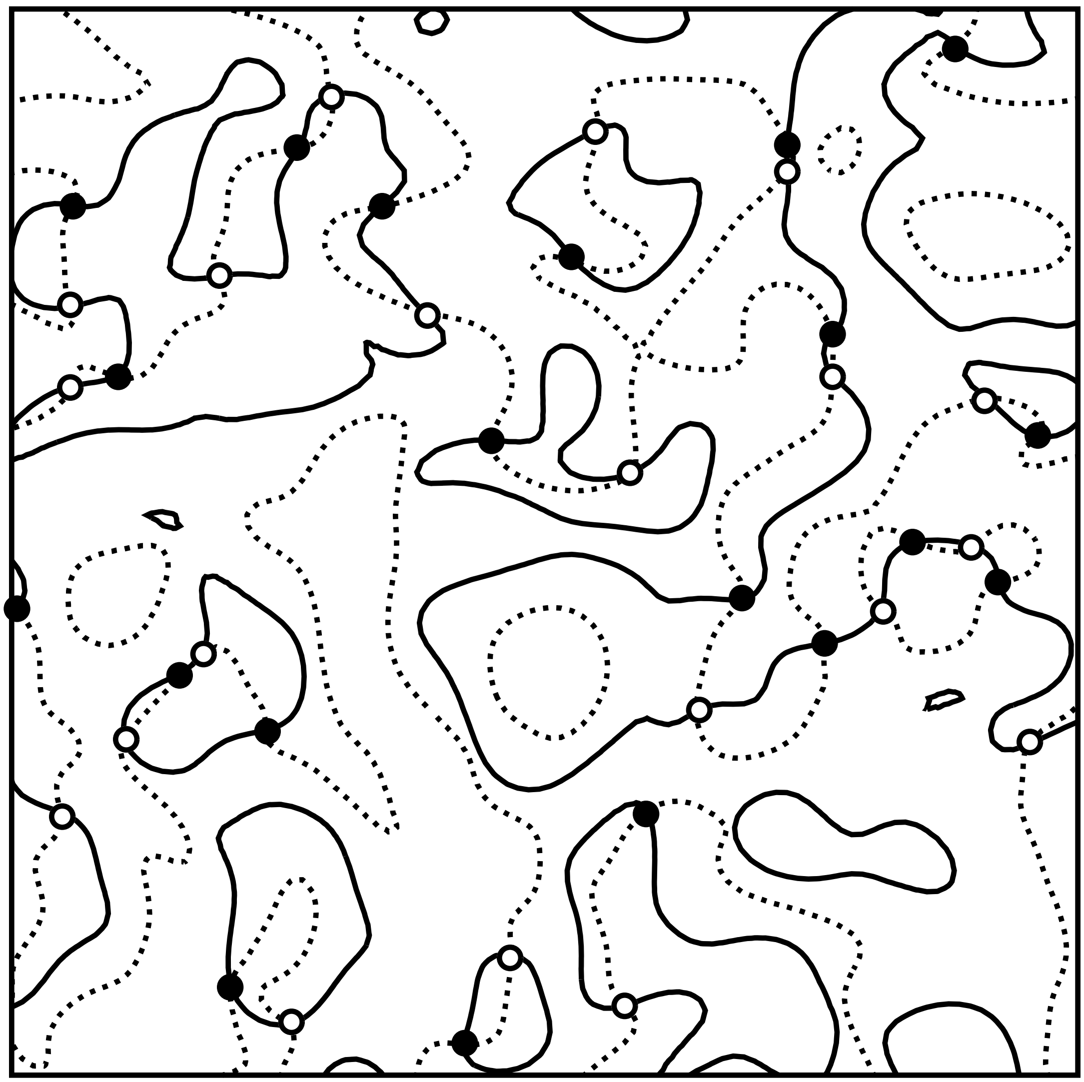

Figure 1

Figure 2

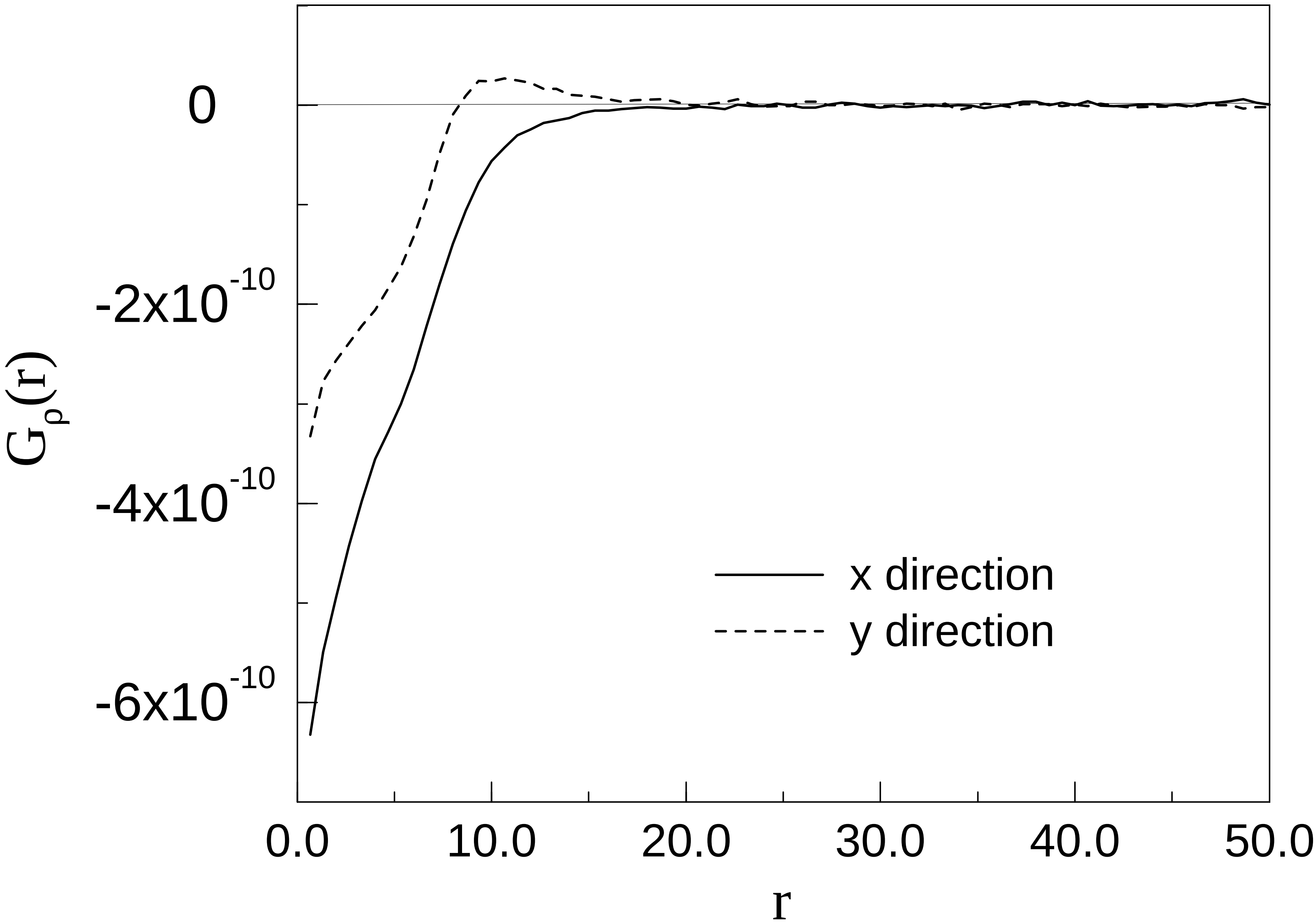

0
-2x10^-10
-4x10^-10
-6x10^-10
Gρ(r)
0.0
10.0
20.0
30.0
40.0
50.0
r
x direction
y direction

Figure 3